ARTICLE IN PRESS

Precipitation enthalpy during cooling of aluminum alloys obtained from calorimetric reheating experiments

Davit Zohrabyan [a,b,*], Benjamin Milkereit [a,b], Olaf Kessler [a], Christoph Schick [b]

[a] *University of Rostock, Faculty of Mechanical Engineering and Marine Technology, 18051 Rostock, Germany*
[b] *University of Rostock, Institute of Physics, 18051 Rostock, Germany*

A R T I C L E   I N F O

A B S T R A C T

Precipitation reactions inside aluminum alloys are known to be very important for hardness and yield strength. Premature precipitation during quenching from solution annealing decreases the yield strength after aging. A methodology to determine the amount of precipitates as a function of quench rate (quench sensitivity) for a wide range of aluminum alloys from calorimetric reheating scans is proposed. The method allows determining the critical cooling rate for suppressing precipitation during quenching. Differential fast-scanning calorimetry was applied to cover the cooling rate range needed for high alloyed materials. The critical cooling rate for the quench sensitive EN AW 7049A alloy was determined as 300 K/s. A new methodology, called differential reheating method, was applied for differential fast-scanning calorimetry (DFSC) and differential scanning calorimetry (DSC). The method was quantitatively verified with EN AW 6063 alloy in a DSC due to its low critical cooling rate. The combination of DSC and DFSC extends the available cooling rate range for precipitation studies from mK/s up to some 10,000 K/s.

© 2011 Elsevier B.V. All rights reserved.

1. Introduction

Knowledge of the properties like yield strength is essential when designing a component, because it generally shows the upper limit of the load that can be applied. Aluminum alloys are generally used because of their preferable strength to weight ratio. High purity aluminum in the annealed condition has very low yield strength of a few 10 MPa. Dislocation movement is the dominant carrier of plasticity. Different types of crystallographic defects can create obstacles for dislocation movement resulting in yield strength increase. Precipitation hardening (age hardening) is a heat treatment method used to increase the yield strength of metals, including alloys of aluminum. Lower solubility of alloying elements with decreasing temperature is a requirement to produce the needed particles. These particles can be introduced in the matrix, in a finely dispersed way, to increase the yield strength [1]. Upon plastic deformation, gliding dislocations in the matrix are obstructed in their movement by these obstacles. In this case two options exist. Either the dislocations cut the particles, or they bow out between particles. The first mechanism prevails for tiny particles coherent with the matrix. If incoherent large particles occur, the governing mechanism is the second one. Further, also solute atoms, other dislocations and grain boundaries disturb the ideal lattice regularity,

thus the dislocations movements can be hindered by these obstacles [1]. As a result yield strengths of some 100 MPa can be achieved with aluminum alloys.

Several investigations of the precipitation processes during aging exist, but only few investigations of the precipitation processes during cooling from solution annealing [2–8]. The Critical Cooling Rate (CCR) [9,10] gives information about the rate where all precipitation reactions are fully suppressed [3,6–8]. After cooling aluminum alloys at the CCR or even faster (overcritical cooling) the maximum hardness value after aging was achieved [3,4,7,8,11]. Depending on the type of aluminum alloy and composition, the CCR can change dramatically (for 6XXX aluminum alloys typically from some 0.1 K/s to some 1000 K/s) [4]. The CCR is commonly obtained from continuous cooling precipitation (CCP) diagrams. However CCP diagrams for aluminum alloys are hardly available. The common recording procedures for steels are not usable and only few other experimental procedures exist. One possibility for recording CCP diagrams of Aluminum alloys is given by differential scanning calorimetry (DSC) [3–5,7,8,12,13]. Due to the fact that modern DSC still has a limited cooling rate range (typically below 10 K/s), aluminum alloys which have CCR higher than the cooling rate range achievable by the device, cannot be studied. [3,5,7,8]. The problem may be solved by the recently developed differential fast-scanning calorimetry [14–16] reaching cooling rates up to 10^6 K/s.

Differential fast-scanning calorimeters are available nowadays e.g. for polymers, but they are not well suited for studying materials like aluminum alloys. The differential fast scanning calorimeter (DFSC) [14], applied here, utilizes extremely small samples in

* Corresponding author at: University of Rostock, Faculty of Mechanical Engineering and Marine Technology, 18051 Rostock, Germany.
   E-mail address: david.zohrabyan@uni-rostock.de (D. Zohrabyan).
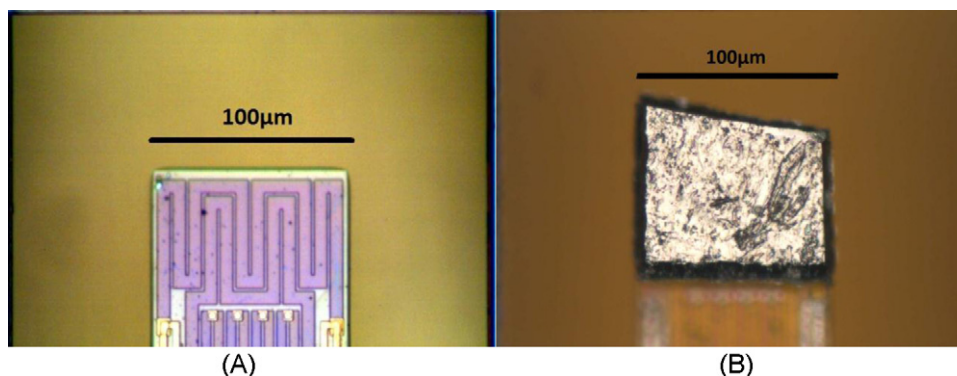
ARTICLE IN PRESS

Fig. 1. EN AW 7049A alloy, light microscope image illustrating the sensor structure (A) and a sample on the sensor (B), sensor type: XI-377 from Xensor Integrations, NL.

dimension of some 10 μm. This small sample dimensions give the possibility to reach faster cooling rates than in conventional DSC, because sample and addenda heat capacity and maximum possible cooling rate are dependent. This article presents first experiments utilizing DFSC for studying precipitation reactions in high alloyed aluminum alloys. After a direct measurement on cooling was not successful a new method was developed, based on reheating experiments, to study the precipitation reactions over a wide cooling rate range from 1 to 3000 K/s. This covers the cooling rate range where also for highly alloyed materials no precipitation occurs.

2. Experimental

2.1. Materials

Aluminum alloy EN AW 7049A (AlZn8MgCu) has a high content of alloying elements and precipitation heat is expected to be large. Further this alloy is known to have a high critical cooling rate [1]. It is therefore a good candidate for fast-scanning experiments. EN AW-1050 commercially pure aluminum with an aluminum mass fraction of more than 99.5% was used as reference material. No precipitation reactions are detectable for this material in the temperature range of interest. EN AW-6063 alloy with a low content of alloying elements and a CCR of about 1.5 K/s was used to test the newly developed reheating method in a conventional DSC, as discussed later. The compositions of the alloys are given in Table 1.

2.2. Methods

Highly alloyed aluminum materials with high CCR require calorimeters which can cool very fast, in order to be able to follow the rapid precipitation reactions which are taking place inside the materials. Fast cooling and heating can only be achieved using extremely small samples. Sensors which are used in the differential fast-scanning calorimeter are based on silicon nitride membranes, because they have a low addenda heat capacity. Scanning rates up to 1,000,000 K/s can be realized, but the devices have low sensitivity below 100 K/s. Due to the flat sensor surface, the sample has to be flat too, for better contact with the sensor. Samples with the required geometry can be prepared with a scalpel from larger pieces under a microscope. The sample preparation consists of several stages: cutting small piece from bulk material, adjusting the sizes

of the sample for the used DFSC sensor, and surface optimization for better thermal contact. Small samples of EN AW-7049A with lateral dimensions (ca. 100 μm × 90 μm × 20 μm) were prepared this way and later placed on the sensor surface (Fig. 1).

After sample preparation the sample loaded sensor and an empty sensor (reference) are connected to the electronic system, which provides the needed power to the heaters of the sensors. The differential fast-scanning calorimeter is intended to measure the heat flow rate into the sample as the power difference between the empty and the sample loaded sensor during fast temperature scans on heating and on cooling at controlled rates. The power difference is recalculated from the remaining temperature difference between sample and reference sensor. For details of the device see [14,17]. The device has an effective working range of controlled heating and cooling in between ($100–10^6$ K/s). Unfortunately at lower rates (below ∼300 K/s) the signal to noise ratio is reduced. Very fast analog to digital converters allows very fast data acquisition rates up to some 100,000 points per second, in case that the processes being studied are very fast. In the presented curves always more than 10 points per Kelvin are collected.

Fig. 2 shows as an example of a typical thermal signal from a differential fast-scanning calorimeter experiment data from a high purity zinc sample. The sample was heated and cooled to show how the signal looks like and to check temperature calibration. Fig. 2 shows the remaining temperature difference between reference and sample sensors, which is proportional to the differential heat flow rate, at heating and cooling at 60 K/s. At these low rates the curve is noisy and only the sharp melting and solidification peaks are clearly seen.

DFSC should allow reaching the critical cooling rate, where precipitation does not occur, even for high alloyed materials. But low
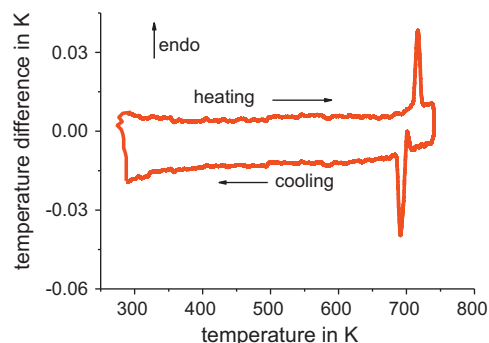
Table 1
Alloying elements contents of the used aluminum alloys.

Mass fraction in %	Si	Fe	Cu	Mn	Mg	Cr	Zn	Ti
EN AW-1050 (ref)	0.09	0.32	0.002	0.004	0.001	0.001	0.01	0.004
EN AW-7049A	0.25	0.35	1.90	0.20	2.90	0.22	8.2	0.10
EN AW-6063	0.6	0.35	0.10	0.10	0.9	0.10	0.10	0.10

Fig. 2. DFSC heating and cooling scans of a high purity zinc sample showing melting and solidification peaks. The zinc particle (ca. 30 μm × 20 μm × 25 μm) was placed on the sensor and scanned between ambient temperature and 740 K heating and cooling rate was 60 K/s.
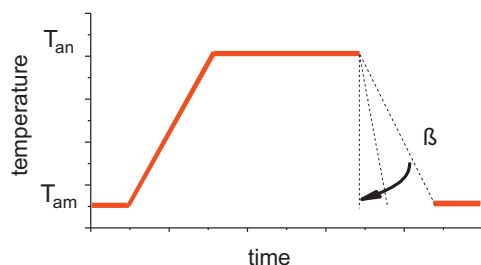
Fig. 3. DFSC program which shows the heat treatment steps, where the sample is solution annealed and cooled with different rates.

sensitivity at lower cooling rates (300 K/s and less) does not allow distinguishing between noise and very small thermal effects. Nevertheless a sample of the aluminum alloy 7049A shown in Fig. 1(B) was used to check the possibilities of DFSC for determining its critical cooling rate. First, the temperature program of Fig. 3 has been used. The sample is solution annealed at 470 °C for 30 min and then cooled with different rates. The outcome of the experiments is shown in Fig. 4.

The Experimental data presented in Fig. 4 gives no useful signals regarding precipitation reactions inside the sample during cooling. In the investigated cooling rate range between 10 K/s and 300 K/s precipitation reactions of EN AW 7049A were expected because the CCR was estimated to less than 1000 K/s [1]. But the typical exothermic precipitation reactions occurring during cooling are not present in these curves. The reason why precipitation is not seen can be:

- Too low signal to noise ratio (low sensitivity at scanning rates below 300 K/s).
- Insufficient and unstable thermal contact between sample and sensor causing bad signals as seen for the curves at 10 K/s and 100 K/s.

Until now these problems have not been solved sufficiently. Therefore direct investigations on cooling were stopped and other possible measurement procedures were discussed. One way to overcome the existing technical problems is to study the dissolution of precipitates formed on previous cooling during reheating. In Fig. 5, the change in enthalpy with temperature for cooling and reheating cycles of an aluminum alloy is shown schematically for relatively fast reheating rates. When the system is slowly cooled from point (1) (solution annealing temperature) precipitation occurs and at point (2) a low enthalpy state is reached. If the sample is reheated immediately after slow cooling back to the
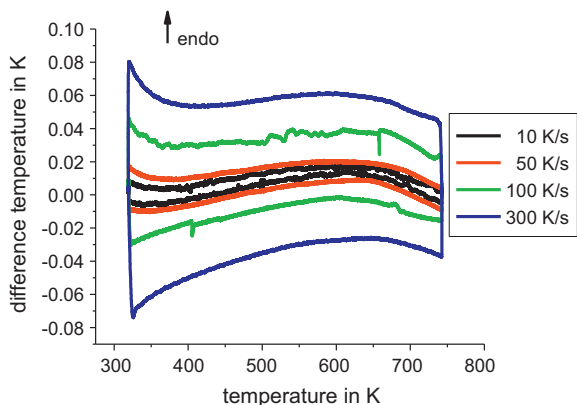

Fig. 4. EN AW 7049A alloy, experiments performed with DFSC. The figure shows heating and cooling scans at different rates.

annealing temperature (point (2) to point (1)), additional precipitation may occur but finally all precipitates, including that formed during slow cooling, dissolve.

When the sample is cooled with overcritical cooling rate from point (1) to point (3), during cooling nothing is precipitating, because there is not enough time for nucleation and growth of the precipitates. Immediate reheating from point 3 back to the annealing temperature (point (1)) shows some thermal effects due to precipitation and dissolution on slow heating. The scheme shown in Fig. 5 consists out of two closed loops in temperature – starting and ending at the solution annealing temperature (point (1)). If we assume that independent on the temperature path the same thermodynamic state is reached at the annealing temperature after reheating (point (1)) then the total enthalpy change for both cooling–reheating cycles equals zero (closed loop).

The enthalpy change on cooling and on heating equals the integral of the heat capacity. As the cooling and reheating processes are taking place in closed loops regarding temperature and enthalpy, one can obtain the total enthalpy changes as the sum of the integrals of the heat capacities of the different parts of the cooling and reheating processes.

Based on a few assumptions we have developed a method allowing determination of precipitation heat on cooling from two reheating scans as detailed next.

Considering a closed thermodynamic cycle where the starting and the end point are in equilibrium, the total enthalpy change equals to zero, Eq. (1).

$$\oint H \, dT = 0 \tag{1}$$

Eq. (1) holds for a closed cycle with slow cooling, when precipitation occurs on cooling, as well as for a cycle where cooling is overcritical. Rewriting the closed loop integral as the sum of the two parts – cooling and heating – one gets

for slow cooling, $\quad \Delta H_{SC} + \Delta H_{HSC} = 0 \tag{2}$

and for overcritical cooling, $\quad \Delta H_{OC} + \Delta H_{HOC} = 0 \tag{3}$

where ΔH_{SC} – enthalpy change for the slow cooling step, ΔH_{HSC} – enthalpy change for the reheating step No1 in Fig. 6, after slow cooling, ΔH_{OC} – enthalpy change for the overcritical cooling step, and ΔH_{HOC} – enthalpy change for the reheating step No2 in Fig. 6, after overcritical cooling.

Neglecting the contributions from the phononic heat capacity and considering only excess heat capacities as exemplified in Fig. 5 one can express the enthalpy terms in Eqs. (2) and (3) as given in Eq. (4) where T_{an} – solution annealing temperature and T_c – subzero temperature to which the sample was cooled.

For slow cooling : $\quad \Delta H_{SC} = \int_{T_{an}}^{T_c} C_{p_{SC}} \, dT \tag{4}$

For reheating No1 (HSC) : $\quad \Delta H_{HSC} = \int_{T_c}^{T_{an}} C_{p_{HSC}} \, dT$

For overcritical cooling (OC) : $\quad \Delta H_{OC} = \int_{T_{an}}^{T_c} C_{p_{OC}} \, dT$

For reheating No2 (HOC) : $\quad \Delta H_{HQC} = \int_{T_c}^{T_{an}} C_{p_{HOC}} \, dT$

The corresponding excess enthalpy curves are presented in Fig. 5.
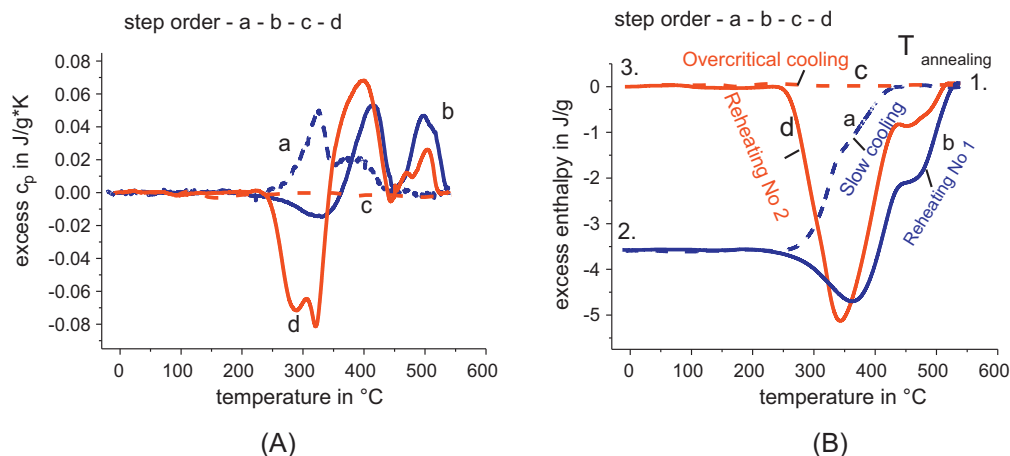
ARTICLE IN PRESS

Fig. 5. (A) Measured excess heat capacity curves from Pyris-1 DSC (Perkin Elmer) for the above discussed two closed loops for EN AW 6063 alloy. Curves: (a – blue, dashed) slow cooling at 0.03 K/s to −20 °C after solution annealing at 540 °C for 20 min, (b – blue, solid) reheating from −20 °C at 0.3 K/s to the solution annealing temperature after (a), (c – red, dashed) overcritical cooling from 540 °C at 6 K/s to −20 °C, (d – red, solid) reheating from −20 °C at 0.3 K/s to solution annealing temperature 540 °C after (c). (B) Excess enthalpy as a function of temperature from the curves shown in (A). (For interpretation of the references to color in this figure legend, the reader is referred to the web version of this article.)

For overcritical cooling, when no precipitation occurs, the excess heat capacity equals zero, see Fig. 5(A), and consequently $\Delta H_{OC} = 0$. The difference of Eqs. (2) and (3) then yields:

$$\Delta H_{SC} = \Delta H_{HSC} - \Delta H_{HOC} \tag{5}$$

where ΔH_{SC} equals the precipitation heat at cooling rates below the critical cooling rate. ΔH_{SC} becomes zero at the critical cooling rate and therefore from ΔH_{SC} as function of cooling rate the critical cooling rate (CCR) is available. Substituting the enthalpy terms on the right hand side by the heat capacity integrals Eq. (5) results in:

$$\Delta H_{SC} = \int_{T_c}^{T_{an}} C_{p_{HSC}}\,dT - \int_{T_c}^{T_{an}} C_{p_{HOC}}\,dT = \int_{T_c}^{T_{an}} C_{p_{HSC}} - C_{p_{HOC}}\,dT \tag{6}$$

The precipitation heat at slow cooling, ΔH_{SC}, is therefore available from the difference of the reheating excess heat capacity curves as expressed in Eq. (6). But Eq. (6) only holds if three conditions are fulfilled:

(i) the cooling starts at a temperature where the sample is in equilibrium and heating ends at the same temperature and equilibrium is reached again. Before cooling, i.e. after solution annealing, equilibrium is reached for most alloys but after reheating, this does only hold if precipitates are highly unstable and fully dissolve during heating. Therefore this approach is valid only for cooling close to critical cooling rate when only small precipitates are formed. Nevertheless, it should allow determining the critical cooling rate.

(ii) The overcritical cooling must be for sure overcritical. Only then $\Delta H_{OC} = 0$ is true and Eq. (6) is valid. For the DFSC experiments this will not be a serious problem because cooling rates of at least 100,000 K/s are possible and this should be faster than the critical cooling rate for common aluminum alloys.

(iii) During the isotherm after cooling at the lowest temperature no precipitation occurs. For high alloyed samples this may be a problem particularly after overcritical cooling because then the sample is in a very unstable state. To avoid precipitation at T_c the time spent at T_c should be short and T_c should be as low as possible to slow down precipitation. For the DFSC experiments these conditions are easily fulfilled, the soaking time is of order 0.01 s and T_c can be as low as −170 °C.

It should be mentioned that the above arguments and calculations hold in the same way also for heat capacity (including phononic heat capacity) and not only for excess quantities if phononic heat capacity is not influenced by the precipitates. Therefore it does not matter if or if not a reference sample compensating for the phononic heat capacity is placed on the reference sensor. Furthermore Eq. (6) can be applied not only to heat capacity curves but to heat flow data or other measured quantities too, if the same sample and the same heating rate is used for both reheating steps, and the measured quantities are proportional to heat capacity. An example for this is given in Figs. 8 and 9 below.

The temperature time profile used for the differential reheating method is shown in Fig. 6. A first cycle consisting of slow cooling (SC) and first reheating (HSC) and a second cycle consisting of overcritical cooling (OC) and second reheating (HOC) are conducted. The two reheating steps are always performed at the same heating rate to allow an easy data evaluation. The heating rate may be selected according to the instrument used in order to realize maximum sensitivity for reheating. The differential reheating method shown in Fig. 6 compared to the temperature time profile for the direct measurements on cooling as shown in Fig. 3, contains two additional heating steps (Reheat No1 (HSC) and Reheat No2 (HOC)). The excess heat capacity data from these additional steps are finally used to calculate the precipitation heat on slow cooling from equation 6. After solution annealing (Fig. 6, step 3), first cooling starts (Fig. 6, step 4) and intermetallic compounds may start to precipitate. Depending on cooling rate β_x (fast or slow)
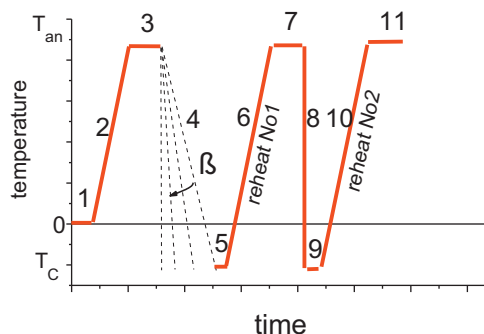

Fig. 6. Modified thermal program, consisting of two additional reheating steps after cooling.
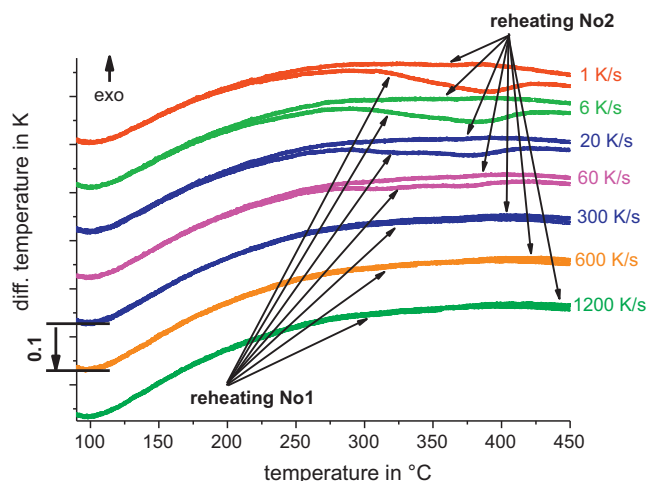
Fig. 7. EN AW 7049A alloy, experiments applying the differential reheating method as described in Fig. 6; first and second reheating vs. sample temperature. The sample was heated to solution annealing temperature held isothermally for 30 min and cooled to ambient temperature with different rates shown in the graph, and then reheated both, first and second, with 1000 K/s rate to solution annealing temperature.

Fig. 8. EN AW 7049 A alloy, results from differential reheating showing the difference between first and second heating as shown in Fig. 7. The sample was solution annealed at 470 °C for 30 min, then cooled with the indicated rate to ambient temperature and reheated with 1000 K/s rate for both heatings to solution annealing temperature.

precipitation intensity changes. When cooling is fast, the degree of precipitation will be less, [3,4,7,8] or more if the cooling is performed slowly. Overcritical cooled samples are in the metastable state of a supersaturated solid solution, so even at ambient temperature some precipitation can start, violating Eq. (6). Cooling to sub ambient temperatures (−20 °C) avoids precipitation at the lowest temperature step 5. Afterwards the sample is reheated with constant rate (Fig. 6, step 6) and solution annealed for the same time as before (Fig. 6, step 7). It is assumed, that during this reheating step the precipitates which have been formed during cooling dissolve, showing an overall endothermic effect. As seen in Fig. 5, if precipitation is not complete on cooling, there may be further exothermic precipitation on heating. But for the applicability of the reheating method this is not important. During the next step (Fig. 6, step 8) the sample is subjected to overcritical cooling, this means that the precipitation reactions are fully suppressed. In this step the sample is cooled also to sub ambient temperatures, step 9. The last step (Fig. 6, step 10) reheating No2 is exactly the same as step 6. Further subtracting the excess specific heat capacity curves or other measured quantities like heat flow rates of the reheating No1 (HSC) in (Fig. 6, step 6) and reheating No2 (HOC) in (Fig. 6, step 10) one can calculate the precipitation enthalpy during step 4 according to Eq. (6).

Before performing a quantitative validation of the reheating method with conventional DSC for a low alloyed aluminum material with low CCR, we checked its applicability to DFSC measurements on precipitation of the aluminum alloy EN AW 7049 A. According the recommended solution annealing conditions for this alloy T_{an} was chosen as 470 °C and t_a as 30 min [18]. Cooling rate was varied in the range from 1 K/s up to 5000 K/s. For the second overcritical cooling step in the scheme of Fig. 6, a cooling rate of 5000 K/s was chosen. The two reheating steps were performed at 1000 K/s, the optimum heating rate for this sample. Heating starts after an equilibration time of 0.05 s at 25 °C. The experimental data, using this method is presented in Fig. 7.

For these experiments the phononic heat capacity was not compensated by a pure aluminum sample on the reference sensor. Consequently, overcritical cooling does not yield $\Delta H_{OC} = 0$. But as briefly discussed above the additional contribution to the measured heat capacity is present in the first reheating too and is canceled out by the subtraction of the first and second heating scans. The
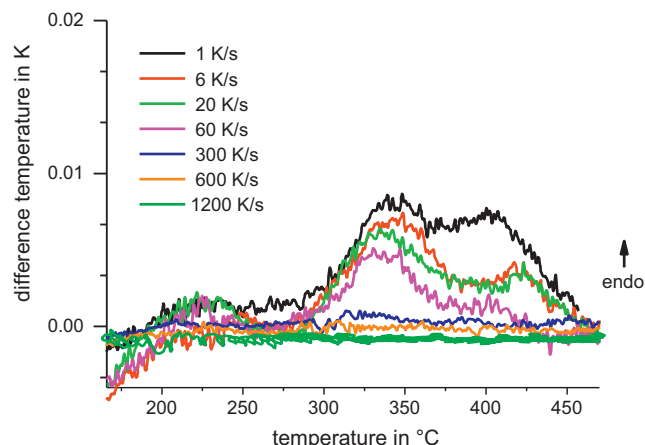
resulting difference curves (first heating–second heating) are shown in Fig. 8. With increasing cooling rate in step 4 of Fig. 6 the difference between the two reheating steps decreases and eventually vanishes. Although these data are only qualitative they verify applicability of the reheating method to obtain information about the precipitation processes in aluminum alloys at cooling.

As known from other aluminum alloys [8], precipitation during cooling proceeds by at least two reactions in different temperature intervals. These two reactions seem also to be visible during reheating of EN AW 7049A, especially after cooling rates in the range of 1–10 K/s. Two partially overlapping peaks occur. The heating rate of 1000 K/s used for the DFSC experiments do not allow further precipitation on heating, but only dissolution. Consequently, the precipitates formed on cooling are dissolving according their stability and size in two distinct temperature ranges.

The integrals (peak area) over the temperature difference curves shown in Fig. 8 provide a qualitative measure of the precipitation heats on cooling and are shown in Fig. 9. The area decreases with increasing cooling rate. For cooling rates above 300 K/s the difference to the overcritical cooling curve at 5000 K/s approaches zero within the error limit of the measurements. For the experimental conditions used here, which are quite unsecure regarding solution annealing temperature (±10 K), the critical cooling rate for the EN AW 7049 A alloy is estimated to 300 K/s. This is in good agreement
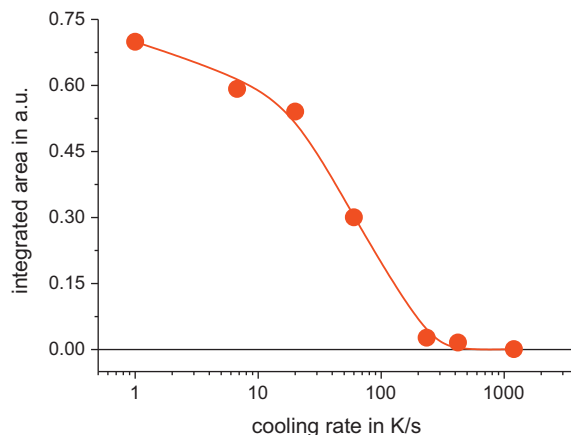

Fig. 9. EN AW 7049A alloy, integration of the curves in Fig. 8. The line is a guide to the eyes only.

with critical cooling rates of other high alloyed 7XXX aluminum alloys (7075, 7178) determined by tension tests in the T6 state after quenching with different rates [1].

From this proof of concept DFSC experiment we conclude that precipitation reactions are traceable at cooling rates far beyond the limits of conventional DSC (ca. 10 K/s) by the newly developed differential reheating method in combination with the DFSC. Nevertheless, before further improving the DFSC reheating method the validity of the basic assumptions as mentioned above must be checked on a quantitative basis.

3. Check of differential reheating method by DSC

For a quantitative check of the reheating method it is useful to compare data from reheating with direct measurements of the precipitation heat on cooling. Precipitation heat on cooling is available from DSC as shown in [3,5,7,8,12,13,19,20]. For the alloy EN AW 7049A, used for the DFSC experiments, the differential reheating method is not applicable at DSC cooling rates (<10 K/s), because cooling cannot be realized at overcritical cooling rate (>300 K/s). But there are other aluminum alloys with a much lower CCR available, which can be used for testing the differential reheating method in a DSC. In [3,4] it was shown that the aluminum alloy EN AW 6063 has a critical cooling rate (CCR) of about 1.5 K/s. Because the available DSC allows cooling up to 3 K/s, step 8 in Fig. 6, can be realized at overcritical cooling rate for this alloy.

For checking the differential reheating method according Fig. 6, we performed experiments with the low alloyed aluminum alloy EN AW 6063 employing a PerkinElmer Pyris-1 power compensation DSC. For this alloy the complete set of precipitation enthalpy data on cooling from slow to overcritical cooling rates are available [3,4,8] and allow a quantitative comparison with the data from reheating. The validation of the reheating method consisted of:

- Determination of the optimal reheating rate for the aluminum alloy EN AW 6063 in the DSC.
- Reheating (with optimal reheating rate) of the aluminum alloy EN AW 6063 samples following the temperature program of Fig. 6 and varying cooling rate in step 4 from 0.01 K/s up to 3 K/s.
- Calculation of the specific precipitation heat from the excess specific heat data out of the two reheating steps according to Eq. (6).
- Comparison of precipitation heat obtained directly on cooling and from the differential reheating method.

First, the optimum heating rate for the temperature profile of Fig. 6 was determined for the employed DSC and the alloy under investigation. Fig. 10 shows the first reheating (step 6, in Fig. 6) of the aluminum alloy EN AW 6063 at different heating rates starting from 0.1 K/s up to 1 K/s. The cooling (step 4 in Fig. 6) in these experiments was kept constant at 0.5 K/s, to observe the influence of the reheating rate. The graph shows that several reactions occur during reheating. At the highest heating rate (1 K/s) the high temperature reaction shifts to higher temperatures and probably does not finalize during the scan, violating the condition of a closed loop in enthalpy as discussed above. But with slower reheating (0.1, 0.3 and 0.5 K/s) the reactions finalize until the end of the scan. This is indicated by the close to zero excess heat capacity at the end of the scan at high temperatures and the shape of the high temperature flank of the high temperature dissolution peak. From the curves shown in Fig. 10 an upper limit for the heating rate of 0.5 K/s is determined. Obviously a lower heating rate would be better because the dissolution peaks are shifted to lower temperatures but the optimum rate has also to be chosen considering the decreasing signal to noise ratio at lower rates. Summarizing, the chosen heating rate
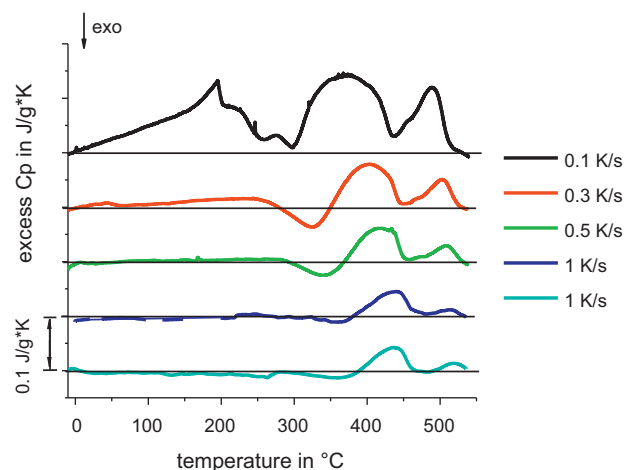

Fig. 10. EN AW 6063 alloy, influence of the reheating rate during first reheating. Sample was subjected to solution annealing at 540 °C for 20 min, then cooled with constant rate 0.5 K/s and then reheated with the rates given in the figure. The two curves with 1 K/s reheating were collected before (blue) and after all other measurements (bottom cyan curve). (For interpretation of the references to color in this figure legend, the reader is referred to the web version of this article.)

must be slow enough to allow all dissolution occurring during the heating scan and it must be fast enough to achieve a good signal to noise ratio. Both conditions are fulfilled at 0.3 K/s heating rate. All reheating experiments (steps 6, and 10, in Fig. 6) were therefore performed at this rate. For all experiments only one sample of EN AW 6063 was used. The reproducibility of the measurements was checked by repeating the experiments after cooling at 1 K/s before and after all other experiments. These two curves are shown in Fig. 10 too, and confirm stability of the sample and reproducibility of the measurements as the reactions peaks are almost the same in the two curves.

The EN AW 6063 sample was reheated with optimal reheating rate up to its solution annealing temperature of 540 °C and kept there for 20 minutes every time. The quenching rate was changed from 0.01 K/s to 3 K/s. The sample was quenched to low temperatures (−20 °C) to avoid precipitation at ambient temperatures.

In Fig. 11 the reheating of the aluminum alloy EN AW 6063 with various quenching rates is presented. As expected the reheating curves are depending on precipitation during cooling. After lower cooling rates only endothermic peaks are seen in the reheating curves. After faster cooling, first an exothermic precipitation peak at reheating is seen. This peak corresponds to precipitation of the alloying atoms not precipitated on fast cooling due to kinetic limitations. It is particularly pronounced at rates near to the critical cooling rate (1.5 K/s). For reheating after very slow cooling the high temperature dissolution is not finalized. At slow cooling very large precipitates are formed [8,19,21] which on heating need relatively long time to fully dissolve. Therefore the method only works for the curves after cooling from 0.1 K/s up to 2 K/s and faster.

The total specific precipitation heat of the reactions on cooling was determined according equation 6 from the curves shown in Fig. 11(B) above. The change in precipitation enthalpy as function of previous cooling rate is shown in Fig. 12. The precipitation enthalpy is high at very slow cooling rates, and becomes small, finally zero at critical cooling rate. The alloy EN AW 6063 has a critical cooling rate of about 1.5 K/s. Therefore the precipitation reactions have been suppressed fully on cooling at higher rates and the integral over the excess specific heat at differential reheating became zero too.

For the alloy EN AW 6063 the precipitation heat on cooling is directly accessible by DSC [4,8]. Fig. 12 shows, for comparison, the precipitation heat on cooling as a solid line. The comparison of the quenching experiments, and reheating data fit perfectly showing
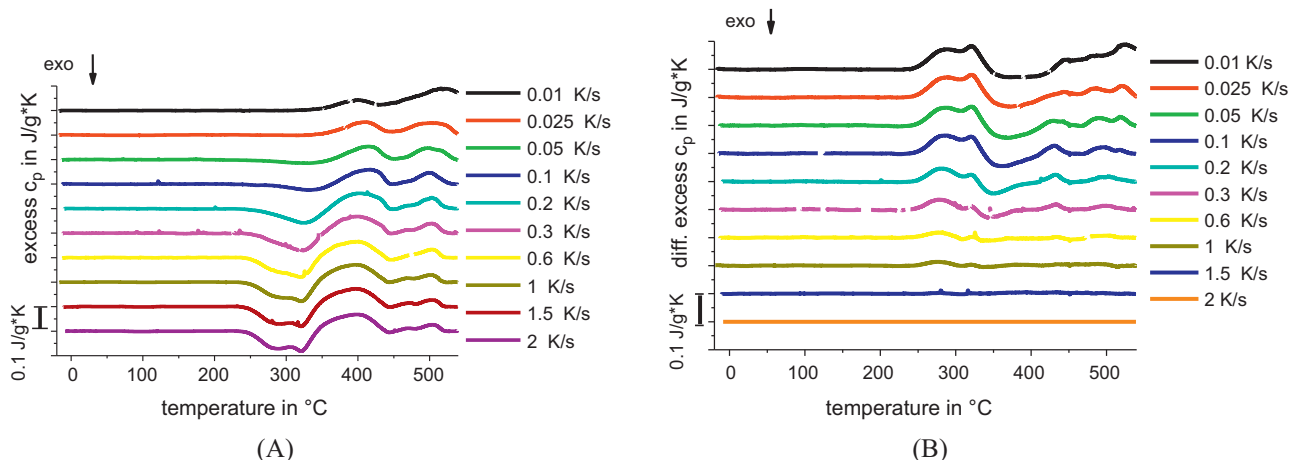
Fig. 11. EN AW 6063 alloy, precipitation/dissolution reactions during first reheating after cooling with different rates (A). Sample was solution annealed at 540 °C for 20 min then cooled with the indicated rates and then immediately reheated with 0.3 K/s. For the differential reheating method (B) the difference between the measured curves in (A) and the reheating curve at 2 K/s are shown. The dissolution reactions visible in (B) are decreasing and finally disappear with increasing cooling rate.
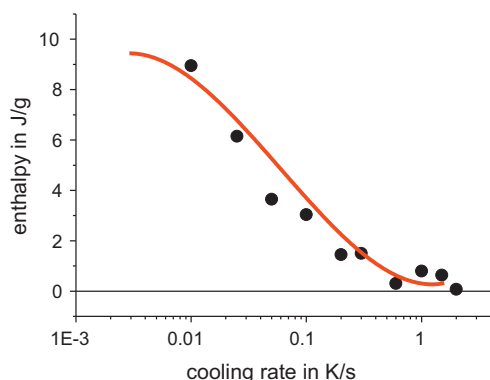

Fig. 12. EN AW 6063 alloy, excess enthalpy from integration of the differential excess c_p curves in Fig. 11(B) as a function of previous cooling rate. Sample was solution annealed at 540 °C for 20 min then cooled with various rates to −20 °C, and reheated with 0.3 K/s. The solid line shows the precipitation enthalpy from cooling data for the same alloy system from [4].

that the reheating method can be used quantitatively to determine precipitation heats on cooling.

4. Summary

The new differential reheating method presented here can be used to characterize the precipitation process during previous cooling of aluminum alloys. The advantages of this method are the following:

- Precipitation monitoring up to critical cooling rate region even for high alloyed aluminum alloys with high critical cooling rates seems to be possible by applying fast scanning calorimetry, e.g. DFSC [14]
- Precipitation enthalpy can be assessed from heating scans collected at optimum experimental conditions without collecting data from the previous cooling step at varying cooling rate.

The prerequisites to be fulfilled for the successful application of the reheating analysis are

(i) a reheating curve after overcritical cooling must be available as a base line, and
(ii) the dissolution of the precipitates must be finalized during the heating scan.

The later condition limits the applicable heating rates as well as the lowest cooling rates because of the stability of the precipitates. But the differential reheating method allows the determination of the critical cooling rate probably for any available aluminum alloy.

References

[1] I.J. Polmear, From Traditional Alloys to Nanocrystals, Elsevier, 2006.
[2] J.L. Cavazos, R. Colás, Quench sensitivity of a heat treatable aluminum alloy, Mater. Sci. Eng. A 363 (1–2) (2003) 171–178.
[3] B. Milkereit, O. Kessler, C. Schick, Continuous cooling precipitation diagrams of aluminium–magnesium–silicon alloys, in: S.B. Hirsch Jr., G. Gottstein (Eds.), Aluminium Alloys, Deutsche Gesellschaft für Materialkunde e.V., WILEY-VCH, Weinheim, Aachen, Germany, 2008, pp. 1232–1237.
[4] B. Milkereit, Kontinuierliche Zeit-Temperatur-Ausscheidungs-Diagramme von Al–Mg–Si-Legierungen, Fakultät für Maschinenbau und Schiffstechnik, University of Rostock, Rostock, 2011, 178 p.
[5] B. Milkereit, M. Beck, M. Reich, O. Kessler, C. Schick, Precipitation kinetics of an aluminium alloy during Newtonian cooling simulated in a differential scanning calorimeter, Thermochim. Acta 522 (1–2) (2011) 86–95.
[6] A. Deschamps, G. Texier, S. Ringeval, L. Delfaut-Durut, Influence of cooling rate on the precipitation microstructure in a medium strength Al–Zn–Mg alloy, Mater. Sci. Eng. A 501 (1–2) (2009) 133–139.
[7] B. Milkereit, O. Kessler, C. Schick, Recording of continuous cooling precipitation diagrams of aluminium alloys, Thermochim. Acta 492 (1–2) (2009) 73–78.
[8] B. Milkereit, C. Schick, O. Kessler, Continuous cooling precipitation diagrams depending on the composition of aluminium–magnesium–silicon alloys, in: 12th International Conference on Aluminium Alloys, The Japan Institute of Light Metals, 2010, pp. 407–412.
[9] A. Takeuchi, A. Inoue, Quantitative evaluation of critical cooling rate for metallic glasses, Mater. Sci. Eng. A 304–306 (2001) 446–451.
[10] J.W. Evancho, J.T. Staley, Kinetics of precipitation in aluminum-alloys during continuous cooling, Metall. Trans. 5 (1) (1974) 43–47.
[11] R.W. Cahn, Combining metals and sciences: ways of investigating intermetallics, Intermetallics 6 (7–8) (1998) 563–566.
[12] T. Herding, O. Kessler, F. Hoffmann, P. Mayr, An approach for Continuous Cooling Transformation (CCT) diagrams of aluminium alloys, in: P.J. Gregson, S. Harris (Eds.), 8th International Conference on Aluminium Alloys: Their Physical and Mechanical Properties, Trans Tech Publications Ltd, Cambridge, UK, 2002, pp. 869–874.
[13] O. Kessler, R.v. Bargen, F. Hoffmann, H.W. Zoch, Continuous cooling transformation (CCT) diagram of aluminum alloy Al–4.5Zn–1Mg, in: W.J. Poole, M.A. Wells, D.J. Lloyd (Eds.), 10th International Conference on Aluminium Alloys, WILEY-VCH, Weinheim, 2006, pp. 1467–1472.
[14] E. Zhuravlev, C. Schick, Fast scanning power compensated differential scanning nano-calorimeter. 1. The device, Thermochim. Acta 50 (1–2) (2010) 1–13.
[15] A.A. Minakov, C. Schick, Ultrafast thermal processing and nanocalorimetry at heating and cooling rates up to 1 MK/s, Rev. Sci. Instrum. 78 (7) (2007) 073902–073910.

[16] S.A. Adamovsky, A.A. Minakov, C. Schick, Scanning microcalorimetry at high cooling rate, Thermochim. Acta 403 (1) (2003) 55–63.

[17] E. Zhuravlev, C. Schick, Fast scanning power compensated differential scanning nano-calorimeter. 2. Heat capacity analysis, Thermochim. Acta 50 (1–2) (2010) 14–21.

[18] H. Chandler, Heat Treater's Guide: Practices and Procedures for Nonferrous Alloys, ASM International, 1996.

[19] B. Milkereit, L. Jonas, C. Schick, O. Kessler, Das kontinuierliche Zeit-Temperatur-Ausscheidungs-Diagramm einer Aluminiumlegierung EN AW-6005A, HTM J. Heat Treatm. Mat. 65 (3) (2010) 159–171.

[20] R. von Bargen, O. Kessler, H.W. Zoch, Kontinuierliche Zeit-Temperatur-Ausscheidungsdiagramme der Aluminiumlegierungen 7020 und 7050, HTM Zeitschrift für Werkstoffe, Wärmebehandlung, Fertigung 62 (6) (2007) 8.

[21] B. Milkereit, Kontinuierliche Zeit-Temperatur-Ausscheidungs-Diagramme von Al–Mg–Si-Legierungen, Shaker Verlag, Aachen, 2011.